Cytotoxicity and effectiveness of archetypal Metal-Organic Frameworks (HKUST-1, UiO-66, MIL-53, MIL-125) against coronaviruses (HCoV-229E and SARS-CoV-2)

Orfeas-Evangelos Plastiras, Peggy Bouquet, Cecile Lecoeur, Jeremy Dhainaut, Jean-Philippe Dacquin, Sebastien Royer, Thierry Loiseau, Anne Goffard, Christophe Volkringer

Cytotoxicity and effectiveness of archetypal Metal-Organic Frameworks (HKUST-1, UiO-66, MIL-53, MIL-125) against coronaviruses (HCoV-229E and SARS-CoV-2)

*Orfeas-Evangelos Plastiras[a,b], Peggy Bouquet[c], Cécile Lecœur[b], Jeremy Dhainaut[a], Jean-Philippe Dacquin[a], Sebastien Royer[a], Thierry Loiseau[a], Anne Goffard[b], Christophe Volkringer[a]**

[a] Unité de Catalyse et Chimie du Solide (UCCS), Univ. Lille, CNRS, Centrale Lille, Univ. Artois, F-59000 Lille, France.

[b] Molecular and Cellular Virology, U1019 – UMR 9017 – CIIL - Center for Infection and Immunity of Lille, Institut Pasteur de Lille, Université de Lille, CNRS, INSERM, CHU de Lille, 59000 Lille, France.

[c] Clinical Microbiology Unit, Institut Pasteur de Lille, Lille F-59000, France.

KEYWORDS: Metal-Organic Framework, Cytotoxicity, SARS-CoV-2, HCoV-229E, Coronaviruses

ABSTRACT: In order to use MOFs in virus decontamination processes, four archetypal MOFs with different metal clusters have been chosen: UiO-66 (Zr), HKUST-1 (Cu), MIL-53 (Fe) and MIL-125 (Ti). Five different concentrations (from 0.01 to 1 mg/mL) for each MOF and three different cell lines (Huh7 TMPRSS2, VeroE6 and Vero81.6) were investigated in aqueous medium (DMEM). Moreover, different cytotoxicity assays were evaluated (MTS, Neutral Red and LDH) and critically compared for the first time, with Neutral Red seemingly to be the most appropriate. HKUST-1 was found to be toxic above 0.1 mg/mL for all of the three cell lines, while the other three MOFs appear to be nontoxic, even above 1 mg/mL. Then, their effect against viruses was monitored, mainly for HCoV-229E and SARS-CoV-2, two different coronaviruses that still cause a lot of infection cases and deaths up to now. Following 1 hour contact with the viruses, HKUST-1 (Cu) and MIL-125 (Ti) were able to greatly diminish the viral titer by 86% and 79.2%, respectively, for HCoV-229E, whereas for SARS-CoV-2 HKUST-1 (Cu), MIL-53 (Fe) and UiO-66 (Zr), demonstrated an efficacy of 68.4%, 63.1% and 56.1%, respectively.

1. Introduction

Coronaviruses, belonging to the family of *Coronaviridae* and subfamily of *Orthocoronavirinae*, are single-stranded RNA viruses with a length of 26 to 32 kilobases and consist of four genera: *Alphacoronavirus*, *Betacoronavirus*, *Gammacoronavirus* and *Deltacoronavirus*. HCoV-229E is one of the viruses of the genus *Alphacoronavirus* that causes mild symptoms of common cold in healthy subjects, and more severe forms in immunocompromised and elderly subjects, while Severe Acute Respiratory Syndrome Coronavirus-2 (SARS-CoV-2), a *Betacoronavirus*, is responsible for the Corona Virus Disease of 2019, also known as COVID-19, which was first detected in Wuhan, China in December 2019.[1,2,3]

This disease was declared on 11th of March 2020 by the World Health Organization (WHO) as a global pandemic that has plagued almost all countries, exhibiting 767 million confirmed cases thus far and over 6.9 million deaths from all around the world as of 6 July 2023.[4]

It is known that SARS-CoV-2 is transmitted by aerosol, droplets or contact, with indoor places being of high risk.[5,6] One of the main pathways of the entry of the virus into the host cells is through the fusion of the viral envelop and plasma membrane after attachment of the spike protein (S) to the ACE2 receptor, ACE2 for SARS-CoV-2 and APN for HCoV-229E.[7,8] Specifically, a cleavage of the spike glycoprotein between the S1/S2 junction and S2' takes place with the aid of furin-like proteases for SARS-CoV-2, but the cleavage of the S1/S2 and S2' of HCoV-229E is mediated by trypsin-like serine proteases, that will later allow the entry of the viruses in the host-cells.[9-11] A variety of drugs have been used so as to hinder the effects of SARS-CoV-2 for the patients that ail from COVID-19, in order to help them recover, but none of them is really effective.[1] Also, the development of vaccines has aided in the decline of deaths worldwide.[12,13]

Many classes of materials have been tested against viruses to evaluate their antiviral activity against SARS-CoV-2, such as carbon-based materials like graphene oxide (GO)[14], functionalized fullerenes[15], or nanoparticles based on several metals, like copper, iron, gold, silver or zinc.[16-18] These materials, especially the metal nanoparticles, might pose a health risk due to their high cytotoxicity.

Metal-Organic Frameworks (MOFs) is a class of porous crystalline solids with a hybrid nature, consisting of different combinations of inorganic metals and organic compounds that serve as linkers between the inorganic cores. The easy tunability of the structural and chemical features

of these materials has caught the eye of the scientists worldwide, as they can be applied to many and different fields, such as catalysis, gas capture, separation and biology.[19,20,21,22,23] By delving deeper into the bio-applications of MOFs, four major fields can be distinguished: bio-imaging[24,], bio-sensors[25], drug delivery[26] and cancer therapy[27]. MOFs could be studied as antiviral agents that might replace more cytotoxic materials, such as metal nanoparticles, having also an appeal for other applications and functions.

When applying MOFs for drug delivery or cancer therapy, cytotoxicity studies have to be conducted onto the appropriate cell lines, in order to calculate the maximum safest value that will not cause cell damage. Three routes have been developed for such investigations related to the *in vitro* assessment of cell viability. Oftentimes, tetrazolium salts like 3-(4,5-dimethylthiazol-2-yl)-2,5-diphenyl-tetrazolium bromide (MTT) or 3-(4,5-dimethylthiazol-2-yl)-5-(3-carboxymethoxy-phenyl)-2-(4-sulfophenyl)-2H-tetrazolium (MTS) are used for their conversion into compounds soluble in aqueous solutions, by the mitochondria of viable cells at 37 °C.[28,29,30] A second method that is widely reported in literature for both metals and organic compounds for the *in vitro* cytotoxicity studies is the Neutral Red (NR) assay, which uses a cationic dye (Figure 1) able to be incorporated into lysosomes of the living cells.[31,32,33] The Lactate Dehydrogenase (LDH) assay is a third method corresponding to the release of the homonym enzyme into the culture media by cells that have undergone rupture in their plasma membrane.[34] All these three methods share one common feature by producing colored species which can be determined by spectrophotometric measurements in their appropriate wavelengths. Besides the difference lying on the different metabolomic pathways, it is observed that the first two methods could directly measure the percentage of alive cells, while the last one measures the percentage of dead cells. The cytotoxicity of selected MOFs has been evaluated with the aforementioned methods, in a wide series of

different cell lines like HL-7702 cells[35], A549[36], HaCaT[37], Huh7[38], Vero[29], HepG2 and MCF7[39], SKOV3 and HUVEC[40], J774 and HeLa cells[41] even in adult zembrafish[42] for the *in vivo* studies (Table S1).

From this literature survey, it was reported that UiO-66 (Zr) was concluded as nontoxic above 1 mg/mL in Vero cells, while J774 and HeLa cells seemed to be more susceptible to this MOF, showing toxicity above 0.4 and 0.06 mg/mL respectively. HKUST-1 (Cu) was found toxic at concentrations above 50 μM in HepG2 and MCF7 cells, and above 1.2 mg/mL for zebrafish. As indicated in Table S1, the MTT molecule is related the most used method, but no information can be extracted about the cell lines of Huh7 TMPRSS2, VeroE6 and Vero81.6, which are typically used for the infection tests of HCoV-229E and SARS-CoV-2, in order to assess the virucidal effect of organic compounds or other materials.

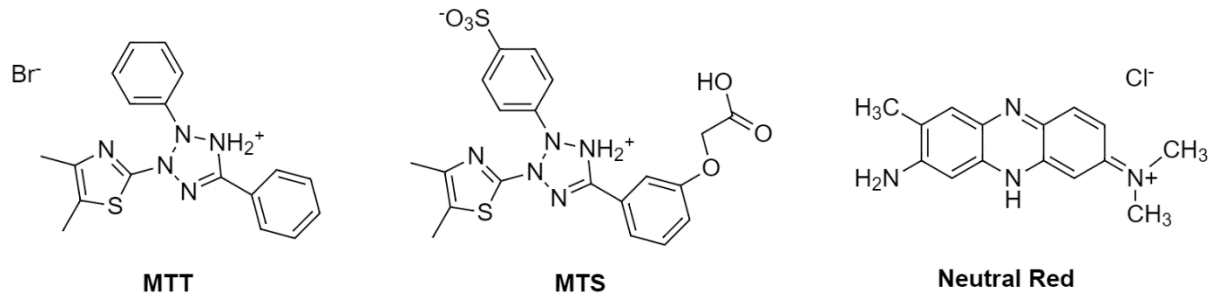

Figure 1. The structural representations of the three species MTT (3-(4,5-dimethylthiazol-2-yl)-2,5-diphenyl-tetrazolium bromide), MTS (3-(4,5-dimethylthiazol-2-yl)-5-(3-carboxymethoxy-phenyl)-2-(4-sulfophenyl)-2H-tetrazolium) and Neutral Red (3-amino-7-dimethylamino-2-methylphenazine hydrochloride) used in the *in vitro* cytotoxicity studies.

For the last two years, very few MOF compounds have also been studied against SARS-CoV-2, evaluating their efficacy and how they can aid to fight the family of virus and the pandemic.[43] Active chlorine was successfully immobilized onto a textile that contained UiO-66-

NH_2, a Zirconium-based MOF, which was able to significantly delay the growth of SARS-CoV-2 after its contact with the nanocomposite textile.[44] Photocatalytic degradation of the virus is also a way to lower its titer, for example UV irradiation or catalysts that get excited by it.[45] MOFs that are able to induce Reactive Oxygen Species (ROS) through their excitation by UV or visible light irradiations are great candidates for that kind of degradation.[46] For instance, zinc-based Zeolite Imidazolate Framework-8 (ZIF-8) was grafted onto face masks in order to hinder the spread of the infection of SARS-CoV-2, and by applying UV radiation for 1 h, a drop of 100% was achieved for the surrogate virus HCoV-OC43, belonging to the *Betacoronavirus* family.[47] In another work, MIL-125(Ti)-NH_2 and MIL-177(Zn)-HT were evaluated as possible antiviral materials against SARS-CoV-2 by adding an amount of them in aqueous solution on top of non-reflective coupons and allowing them to be in contact with the virus.[48] By exposing these both materials to fluorescent light for 30 min, almost 50% reduction of the viral titer was achieved.

As observed, the common techniques that are used to evaluate the effectiveness of the materials against degradation of viruses involve Real Time quantitative Polymerase Chain Reaction (RT-qPCR) and 50% Tissue Culture Infectious Dose ($TCID_{50}$). RT-qPCR measures the amount of viral RNA and therefore does not allow the assessment of infectivity, which is determined by using the $TCID_{50}$ method, where we get information about the possible decrease of infectivity of the virus. Detection of viral protein N using western blot assay confirms the intracellular replication quantified using $TCID_{50}$ method.

In this work, four archetypal Metal-Organic Frameworks, named UiO-66(Zr), HKUST-1(Cu), MIL-53(Fe) and MIL-125(Ti) (Figure 2), were selected based on their large use in the literature as well as their different cationic centers (Ti^{4+}, Fe^{3+}, Cu^{2+}, Zr^{4+}), that could influence the virus degradation.

First, we have conducted cytotoxicity studies in three cell lines, Huh7 TMPRSS2, VeroE6 and Vero81.6 by using three different routes of cytotoxicity tests (MTS, NR and LDH). The aim of this study was to give a comparison of the three types of cytotoxicity assays, determining their accuracy in correctly measuring the cells viability. The MOF compounds are then considered as virucide in the appropriate concentrations, in order to perform tests with two coronaviruses, HCoV-229E and SARS-CoV-2.

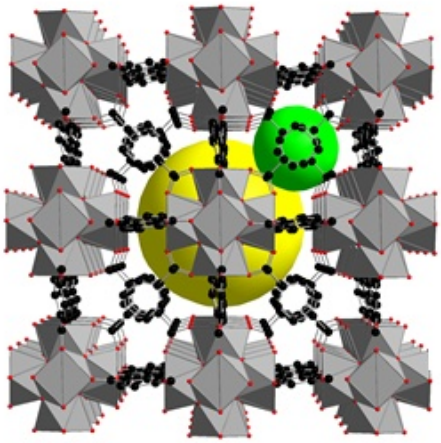

UiO-66 (Zr)

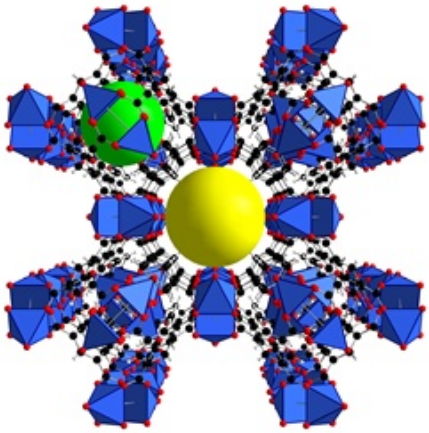

HKUST-1 (Cu)

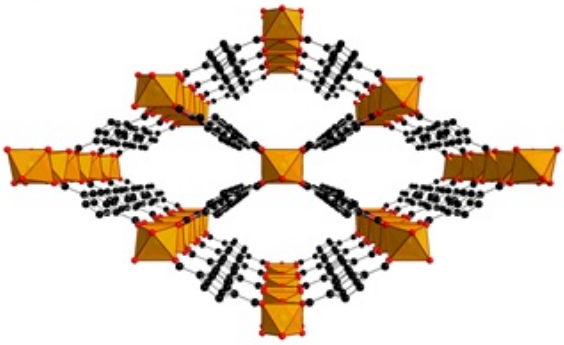

MIL-53 (Fe)

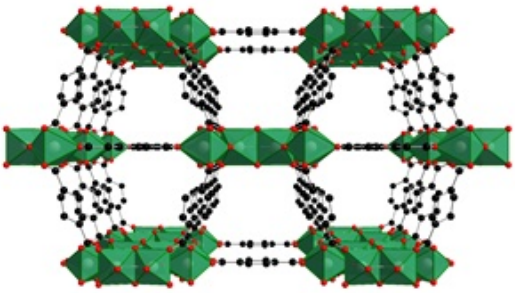

MIL-125 (Ti)/
MIL-125-NH_2

Figure 2. Crystal structural representations of the four MOF archetypes used in this study. Grey refers to UiO-66 (Zr), blue to HKUST-1 (Cu), orange to MIL-53 (Fe), green to MIL-125 (Ti) and to MIL-125-NH_2 (Ti).

2. Experimental section

2.1 Materials, cells and viruses

Zirconium(IV) chloride ($ZrCl_4$, >99.5%), 1,4-benzenedicarboxylic acid (H_2BDC, 98), 2-amino-4-benzenedicarboxylic acid (H_2N-BDC, 99%) copper nitrate hemipentahydrate $(CuNO_3)_2 \cdot 2.5\ H_2O$, 98-102%) and anhydrous N-N-dimethylformamide (DMF) were purchased from Alfa Aesar. Glacial acetic acid and ethanol 96% were bought from VWR. Methanol was bought from Brabant and anhydrous methanol was prepared by putting 50 g of molecular sieves 4 Å in 250 mL of methanol. Iron(III) chloride hexahydrate 97%, titanium tetraisopropoxide 97% (TTIP), 1,3,5-benzenetricarboxylic acid (trimesic acid or BTC), and butyric acid were purchased from Sigma-Aldrich. Dulbecco's phosphate buffered saline (DPBS or PBS) 1X, Dulbecco's Modified Eagle Medium (DMEM) 1X, Trypsin-EDTA 0.05X were bought from Gibco. Fetal Bovine Serum (FBS) was bought from Eurobio. Neutral Red (NR) was bought from Clin-tech, MTS (Cell Titer 96 aqueous nonradioactive cell proliferation assay) was from Promega and the LDH kit (cytotoxicity LDH assay kit-WST) was from Dojindo. Renilla Lysis buffer and the Luciferase reagent were bought from Promega. Polyclonal rabbit anti-SARS-CoV-2 nucleocapsid antibodies for the Western blot were bought from Novus, mouse anti-tubulin was purchased from Sigma-Aldrich and horseradish peroxidase (HRP)-labeled goat-anti-rabbit and goat-anti-mouse IgG antibodies were from Jackson Immunoresearch.

Huh7, VeroE6 and Vero81 (ATCC number CCL-81) were grown in DMEM with 10% FBS in an incubator at 37 °C with 5% CO_2. Vero81 cells were subcloned to obtain a better overall infection rate. HCoV-229E strain VR-740 (ATCC) and recombinant HCoV-229E-Luc (kind gift of V. Thiel) were used.[49] SARS-CoV-2 (isolate SARS-CoV-2/human/FRA/Lille_Vero-81-TMPRSS2/2020; NCBI MW575140) was propagated on Vero81 TMPRSS2 cells.Synthesis and characterization of the MOFs

The detailed synthesis protocols of the MOFs and their characterizations are presented in supplementary information and confirm the purity and the good crystallization of these materials.

2.2 Cell culture and cytotoxicity assay protocols

MTS, NR and LDH assays were used to determine the optimal non-cytotoxic concentrations of the MOFs on Huh7 TMPRSS2, VeroE6 and Vero81.6 cell lines. The preparation of the cells, the stock and working solutions of the MOFs suspensions and the protocols of the three assays are explained in supporting information and were followed as in previous studies.[34, 50]

2.3 Infection tests with HCoV-229E

After the statistical analysis of the data from the cytotoxicity tests, the maximum concentration of the MOFs that had no statistical significance in the growing or the killing of Huh7 TMPRRS2 cells was used, namely 0.1 mg/mL for HKUST-1 (Cu), MIL-53 (Fe) and MIL-125 (Ti) and 1 mg/mL for UiO-66 (Zr). Firstly, Huh7-TMPRSS2 were seeded at 6×10^4 cells/well 24 h before infection in a 96-well plate. The following day, the appropriate dilutions from the stock solutions, which were kept in the fridge at 4 °C for one week, were done from 5 mg/mL of stock solution to 2 mg/mL for UiO-66 (Zr) and 0.2 mg/mL for the other three MOFs in 0.25 mL of

complete medium. HCoV-229E-luc is added to the diluted MOFs for a final volume of 0.5 mL. These tubes were agitated for 1 h at room temperature in a rotating wheel homogenizer (time of contact of the MOF and the virus was 1 h) and subsequently centrifuged for 5 min at 5000 rpm. The medium from the wells was eliminated and the supernatant was collected from the Eppendorf tubes and 0.1 mL was added to each well (3 wells for each MOF, triplicate analysis). Three wells were infected with the virus alone (positive control), and three wells were left untouched (negative control). The plate was incubated for 1 h (37 °C, 5% CO_2) and then the supernatant was eliminated and 0.1 mL of fresh DMEM + 10% FBS was added to each well. Then, the plate was further incubated for 6 h (37 °C, 5% CO_2). After 6 h of incubation, the medium was eliminated, and 0.1 mL of PBS was added to each well to wash them. Then, PBS was discarded and 0.02 mL of Renilla Lysis Buffer, that was previously diluted 1/5 in MilliQ water, was added to each well. The determination of the luciferase activity was done by fluorescence, using the luciferase reagent, by a Tristar LB 941 luminometer from Berthold Technologies (Bad Wildbad, Germany). In Figure 3, a flow diagram of the procedure is visualized.

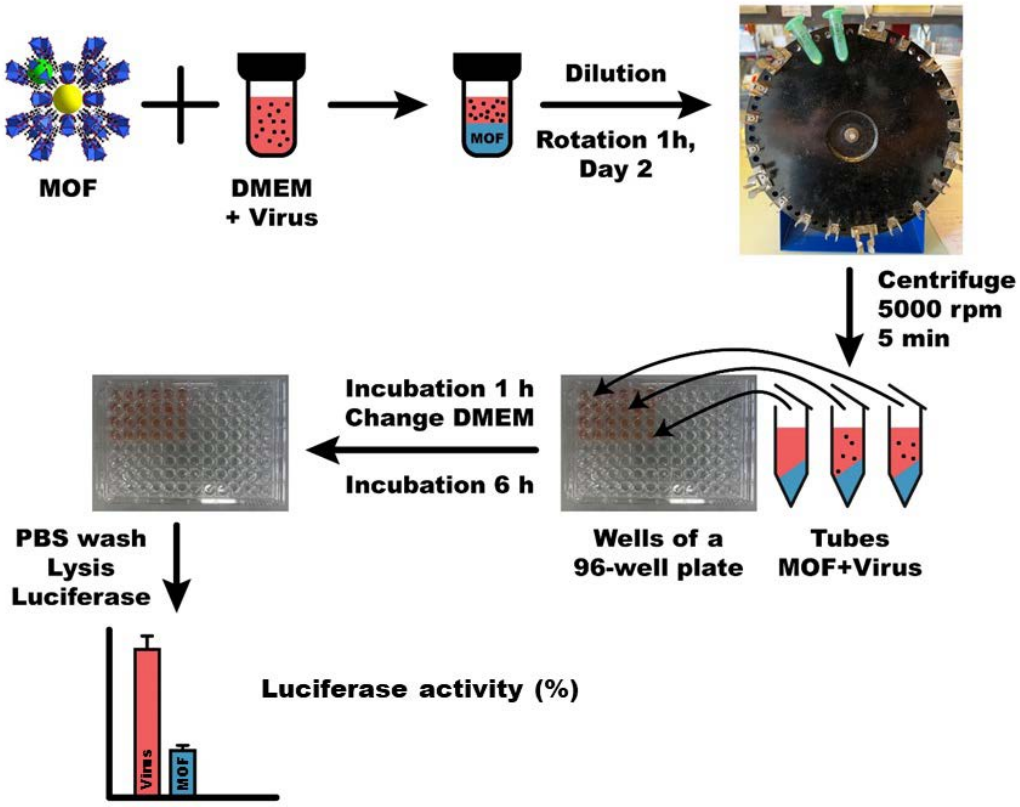

Figure 3. The main steps of preparation and incubation of the MOFs with the virus that is contained in DMEM and its subsequent determination of titer in order to evaluate the efficacy of the materials against HCoV-229E-Luc.

2.4 Infection tests with SARS-CoV-2, Western blot and titer determination protocol

Vero 81 cells expressing TMPRSS2 receptor were seeded in 24-well plates at 2×10^5 cells/well 24 h before infection. The delta variant of SARS-COV-2 was incubated with different concentrations of the MOFs, at a multiplicity of infection (MOI) of 0.01 (arb. unit), during one hour on a wheel in a final volume of 1 mL. The tubes were centrifugated at 5000 rpm for 5 minutes and 500 µL of each supernatant were used to inoculate the cells for 1 h at 37°C, 5% CO_2. The inoculum was removed, and fresh medium was added for 16 h at 37 °C. Due to the handling of

potential lethal virus all experiments involving SARS-COV-2 were conducted in a biosafety level 3 (BSL3) laboratory.

After 16 h of infection, the cells were lysed using reducing Laëmmli loading buffer and inactivated 30 min at 95 °C. Proteins were then separated into a 12% SDS-polyacrylamide gel electrophoresis and transferred on nitrocellulose membranes (Amersham). The membranes were blocked at least 30 min at room temperature using 5% (w/v) of non-fat dry milk in PBS with 0.1% (v/v) of Tween-20. Membranes were then incubated overnight at 4 °C with a polyclonal rabbit anti-SARS-CoV-2 nucleocapsid antibody (Novus) or a mouse anti β tubulin IgG1 antibody (T5201, Sigma). After 3 washes with PBS with 0.1% of Tween-20 (v/v), the membranes were incubated at room temperature with a horseradish peroxidase-conjugated goat anti rabbit IgG antibody (Jackson Immunoreseach). The membranes were then washed 3 times, and the N protein and β tubulin were visualized by enhanced chemoluminescence (PierceTM ECL, ThermoFisher Scientific) on LAS3000 (Fujifilm). The signals were quantified by using the gel function of Image J. The experiment was carried out 3 times in duplicates. Cell supernatants were collected after infection assays with MOFs and the amount of infectious virus was determined by infectivity titration, as discussed before.[51] Therefore, Vero-E6 cells, seeded in 96-well plates, were inoculated with 100 µL of ten-fold serial dilutions of supernatants (ranging from 10^{-1} to 10^{-8} M), eight wells per dilutions were used. Cells were incubated with the virus dilutions for 5 days at 37°C and 5% CO_2. Then, the 50% tissue culture infectious dose ($TCID_{50}$) was determined by assessing the cytopathic effect in each well by light microscopy, and the 50% endpoint was calculated according to the Spearman and Kärber method.

2.5 Statistical analysis

Statistical analysis, to interpret accurately the results obtained from the cytotoxicity tests and from the infection experiments, was performed by using the programming language R (version 4.2.1) and RStudio (version 2022.07.1+554).[52] The cytotoxicity measurements obtained for the 5 concentrations of a MOF and a cell line were compared with an ANOVA (Analysis of Variance) or its non-parametric alternative the Kruskal-Wallis test. The Kruskal-Wallis test was privileged when the homogeneity (Levene's test) or the normality (Shapiro's test) of the data were not observed. When the p value is lower than 0.05 ($p < 0.05$) from the above tests, we declare a significant difference and the post-hoc test of Dunnett (from the package DescTools) or Conover (from the package PMCMRplus) was performed for pairwise comparison to the control group (cells without MOF). All statistical tests are two-sided. For the infection tests, the two-way ANOVA was applied to validate any statistically significant difference in the decrease of the viral titer.

3. Results and discussion

3.1 Evaluation of cytotoxicity assays

After repeating each cytotoxicity assay three times for each cell line (Huh7 TMPRSS2 VeroE6 or Vero81.6), the graphs (Figure 4) were plotted for each MOF with the five different concentrations (0.01, 0.05, 0.1, 0.5 and 1 mg/mL^{-1}), where the mean value of the three experiments, the standard deviations at a confidence level of 95%, and the corresponding p-values (indicated by "*") are shown.

Concerning **Huh7 TMPRSS2 cells**, UiO-66 (Zr), MIL-53 (Fe) and MIL-125 (Ti) show no signs of cytotoxicity up to 1 mg/mL (101.5-123.2%), as seen from the MTS and NR tests. HKUST-

1 (Cu) is cytotoxic at concentrations 0.5 mg/mL and above (9.5-19.5%). Regarding the LDH assay, UiO-66 (Zr) seems to be cytotoxic at 0.05 mg/mL (79.5%), but not at concentrations above this level. Also, HKUST-1 (Cu) demonstrates signs of toxicity at lower concentrations, starting from 0.05 mg/mL (76.6% at 0.05, 61.8% at 0.1, 49.4% at 0.5 and 29.4% at 1 mg/mL). In **VeroE6 cells**, similar results as in Huh7 TMPRSS2 cells are seen (85.8-115.1% from MTS and NR tests, for UiO-66 (Zr), MIL-53 (Fe) and MIL-125 (Ti)), except for HKUST-1 (Cu), that is toxic at 0.1 mg/mL from the NR test (72.2%) and from the LDH test (69.5%). From the MTS assay, HKUST-1 (Cu) is toxic at 0.5 mg/mL (32.1%). LDH gives similar results as the MTS and NR for the other three MOFs. Lastly, in **Vero81.6 cells**, HKUST-1 (Cu) exhibits alike results as in VeroE6, meaning that according to MTS 0.5 mg/mL is the toxic concentration against the cells (59.0%), while with NR 0.1 mg/mL is toxic (75.9%) and with LDH 0.05 mg/mL is enough to show toxicity (56.9%). MTS, NR and LDH are in accordance with the cytotoxicity results shown for UiO-66 (Zr), MIL-53 (Fe) and MIL-125 (Ti), where no sign of toxicity is demonstrated up to 1 mg/mL (89.3-123.2% at 1 mg/mL).

By comparing the three procedures, MTS and LDH assays seem to give high standard deviations in the case of HKUST-1 (Cu) in VeroE6 and Vero81.6 for the former, being 79.2% at 0.01 mg/mL and 75.4% mg/mL in VeroE6, 122.6% at 0.01 mg/mL, 44.1% at 0.1 mg/mL and 34.6% at 0.5 mg/mL in Vero81.6 cells. For the latter method, UiO-66 (Zr), MIL-53 (Fe) and MIL-125 (Ti) demonstrate the highest standard deviations in all 3 cell lines. Specifically, UiO-66 (Zr) shows 36.1% at 0.01 mg/mL and 34.9% at 0.5 mg/mL in Huh7 TMPRSS2 cells, 169.3% of deviation at 0.5 mg/mL in VeroE6 cells and 57% at 0.01 mg/mL and 45% at 0.5 mg/mL in Vero81.6 cells. MIL-53 (Fe) exhibits 36% of standard deviation at 0.01 mg/mL in Huh7 TMPRSS2 cells, 39.9-145.6% for all five concentrations in VeroE6 cells (except at 0.5 mg/mL, whose value

is 10.3%), and 54.8% at 0.05 mg/mL in Vero81.6 cells. Lastly, MIL-125 (Ti) demonstrates deviations ranging from 26.4% to 54.5% for the first three concentrations in Huh7 TMPRSS2 cells, 25.9%-108.8% for all five concentrations in VeroE6 cells and 23.3%-55.1% for the first two and last two concentrations in Vero81.6 cells. On the other hand, standard deviations that are calculated from the NR assay experiments range from 0.4-12.4% in Huh7 TMPRSS2 cells, 0.4-14.5% in VeroE6 cells and 4.5-25.2% in Vero81.6 cells, for all five concentrations and for all four MOFs, rendering this assay as the most precise of the three, when it comes to the assessment of cytotoxicity of MOFs. Similar results about high standard deviations obtained from the LDH and MTS test were also observed in other studies.[34, 53]

Another problem that arises from the MTS and LDH method, is that sometimes very high mean values appear. In detail, low concentrations of HKUST-1 (Cu), from 0.01 to 0.1 mg/mL, give relatively high values in the MTS assay in the last two cell lines, them being between 161.7-184.8% in VeroE6 and between 143.6-195.1% in Vero81.6 cells. These huge values would suggest that low doses of HKUST-1 (Cu) could attribute to the increase of produced cells in these cell lines, something that is not evident with the NR assay. A possible explanation could be that HKUST-1 (Cu) interferes in the redox reaction that takes place for the MTS compound, acting as a catalyst that reduces it synergistically with the cofactors that are responsible in the mitochondria of alive cells. Concerning the LDH test, abnormal high mean values are observed in VeroE6 cells, at 0.1 mg/mL for MIL-53 (Fe) and MIL-125 (Ti), being 181.3% and 183.5% respectively, and at 0.5 mg/mL for UiO-66 (Zr), being 204.8%. Once again, these MOFs could have an impact on the redox reaction concerning the LDH molecule and VeroE6 cells. The NR assay seems to give similar results with the MTS test about the toxicity of HKUST-1 (Cu) in the last two concentrations, which range from 17.6% to 59% for the MTS and from 9.5%-16.7% for the NR,

indicating its cytotoxicity for the three cell lines. Also, NR seems to be in accordance with MTS for the highest concentration of the other three MOFs, exhibiting values that range between 98.1-123.2% (MTS) and 89.3-105.6% (NR) for UiO-66 (Zr), 106.5-123.2% (MTS) and 85.8-105.6% (NR) for MIL-53(Fe), 109.8-116.4% (MTS) and 92.1-110.7% (NR) for MIL-125 (Ti) for all three cell lines. Higher values than 100% were also for other molecules in previous studies, that confirm the variation of our obtained results.[34, 54]

In conclusion, the LDH assay gives variable (from 3.8% to 145.6%) and not accurate results for most of the concentrations tested, probably due to its complex nature of redox reactions that take place. While the MTS test and NR assay present similar results for most of the concentrations tested, the former exhibits higher standard deviations from the NR, while also being false for low concentrations of HKUST-1 (Cu). Considering that NR is the most accurate and precise among the three, the three cell lines seem to be able to tolerate UiO-66 (Zr), MIL-53 (Fe) and MIL-125 (Ti) in concentrations ranging from 0.01 up to 1 mg/mL, while HKUST-1 (Cu) becomes toxic for Huh7 TMPRRS2 cells above 0.1 mg/mL and above 0.05 mg/mL for VeroE6 and Vero81.6 cells. In Table 1, the highest safest concentrations that do not show cytotoxicity (meaning values above 80%) and that can later be used for the infection test are presented for each cell line, according to the results of the NR assay. Furthermore, the cytotoxicity of MIL-125(Ti)-NH_2 was calculated by the NR assay with the same method used for the other four archetypal MOFs, and its results can be seen in Figure S5.

Among these results we observe a dose-dependent trend in HKUST-1, not observed in the other three MOFs. This observation confirms previous studies reported in literature about MOF cytotoxicity.[37] This behaviour is assigned to the specific cytotoxicity of copper, compared to the other metals (Ti, Fe, Zr).[34,36]

Taken all the above into account, for HCoV-229E 1 mg/mL will be used for UiO-66 (Zr) and 0.1 mg/mL for HKUST-1 (Cu), MIL-53 (Fe) and MIL-125(Ti). For SARS-CoV-2, 0.1 mg/mL is the maximum safest concentration of HKUST-1 (Cu), while the other three aforementioned MOFs, with MIL-125(Ti)-NH_2, will be used at 1 and 5 mg/mL.

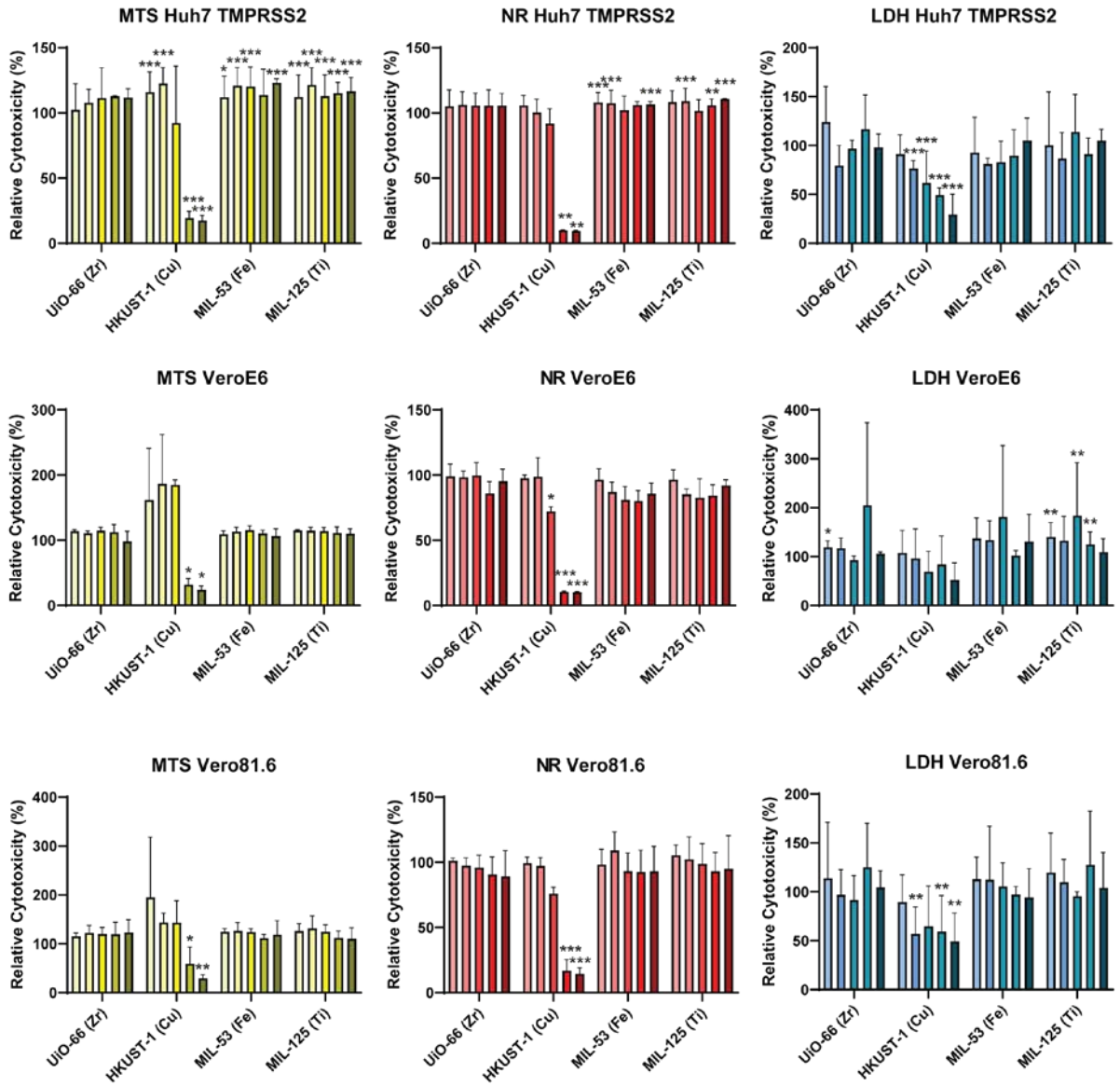

Figure 4. Results from the three cytotoxicity assays for the four MOFs that were studied in five different concentrations and in three cell lines (Huh7 TMPRSS2 VeroE6, Vero81.6). Relative

cytotoxicity (%) refers to the ratio between the measurement of the absorbance of each MOF divided by the one of the control. Concentrations tested were between 0.01 and 1 mg/mL, from the light colored to the darker, respectively. * for $p < 0.05$, ** for $p < 0.01$ and *** for $p < 0.005$ as obtained after the statistical analysis.

Table 1. A summary of the highest safest concentration of each MOF for each cell line, according to the results of the NR assay.

MOF	**Cell line**	**Highest Safest Concentration**	**Cytotoxicity values expressed in $\bar{x}$ (%) $\pm$ s (%)**	**Concentration compared to literature**
UiO-66 (Zr)	Huh7 TMPRSS2	1 mg/mL	105.6 ± 9.3	>1 mg/mL (Vero)[44]
	VeroE6		95.4 ± 9.2	
	Vero81.6		89.3 ± 19.9	
HKUST-1 (Cu)	Huh7 TMPRSS2	0.1 mg/mL	91.8 ± 11.4	-
	VeroE6	0.05 mg/mL	98.7 ± 14.5	
	Vero81.6	0.05 mg/mL	97.3 ± 17.3	
MIL-53 (Fe)	Huh7 TMPRSS2	0.1 mg/mL	102.1 ± 10.9	-
	VeroE6	1 mg/mL	85.8 ± 8.1	
	Vero81.6	1 mg/mL	93.1 ± 19.1	
MIL-125 (Ti)	Huh7 TMPRSS2	0.1 mg/mL	101.5 ± 8.7	-
	VeroE6	1 mg/mL	92.1 ± 4.3	
	Vero81.6	1 mg/mL	95.1 ± 25.2	

3.3 Results from the infection tests with HCoV-229E

The concentrations of the MOFs that were used for the infection tests against HCoV-229E were 1 mg/mL for UiO-66 (Zr) and 0.1 mg/mL for HKUST-1 (Cu), for MIL-53 (Fe) and MIL-125 (Ti), as these concentrations were considered not toxic. Three experiments were also performed in

order to evaluate the efficiency of our four selected MOFs against the inactivation of *Alphacoronavirus* HCoV-229E, under visible light from the lamps of the lab (fluorescent tube, 36 W, 3350 lumens, white light) at room temperature. Two different controls were made so as to be able to observe the effect of the MOFs, mainly a control virus without it being in contact with a MOF, and a cells control, where no virus was added in the wells. The results of the luciferase activity are summarized in Figure 5. Only HKUST-1 (Cu) and MIL-125 (Ti) showed a great decrease in the infectivity of the virus, being 86% and 79.2% respectively. MIL-53 (Fe) and UiO-66 (Zr) show a lesser effect on the virus, reducing its infectivity by 41.2% and 16.4% respectively.

~~The effect of HKUST-1 (Cu) could be attributed to its metal center of Cu(II) that can undergo redox reactions and that can form reactive oxygen species (ROS), that impair the viral envelope's proteins.~~ The release of copper cations Cu^{2+} in the solution cannot be ruled out, since this solid in known to be sensible to hydrolysis[57], as seen from the PXRD patterns and the SEM images (Figure S6, S7). So far, the mechanism reducing coronaviruses activity is not clear in the literature, and suggest that coronaviruses degradation can find its origin from protein of the viral envelop[55, 56] or from the viral RNA[58]. Then, based on the antimicrobial activity of copper, we can propose two paths that could explain the better efficiency of Cu-based MOF. The effect of HKUST-1 could be attributed to its metal center of Cu(II) that can undergo redox reactions and that can form reactive oxygen species (ROS), that impair the viral envelope's proteins. The second possibility, involve release of copper ions in the solution, diffusing within virus and degrading RNA.[58]

Titanium oxide (TiO_2) was used as a thin-film coating in borosilicate glass substrates against HCoV-229E and no drop on the viral titer was observed in that case.[59] However, MIL-125 (Ti) that consists of Ti_8 clusters is known to have a catalytic effect on organic compounds, that could explain its efficacy against HCoV-229E.[60, 61]

MIL-53 (Fe) is built up from Fe(II)/Fe(III) as its metal group, which is responsible for generation of hydroxyl radicals that can attack the viral envelope *via* Fenton-like reactions.[62, 63] UiO-66 (Zr) low effect could be attributed to its Lewis acidity, that probably is not so strong to attack the virus as the ROS that could be produced from the other MOFs. Concluding, HKUST-1 (Cu) and MIL-125 (Ti) show the best results of the four MOFs against HCoV-229E at concentrations of 0.1 mg/mL and indicate that the infectivity of the virus is decreased. Further analyses should be performed in order to find out the mechanism of action of these materials.

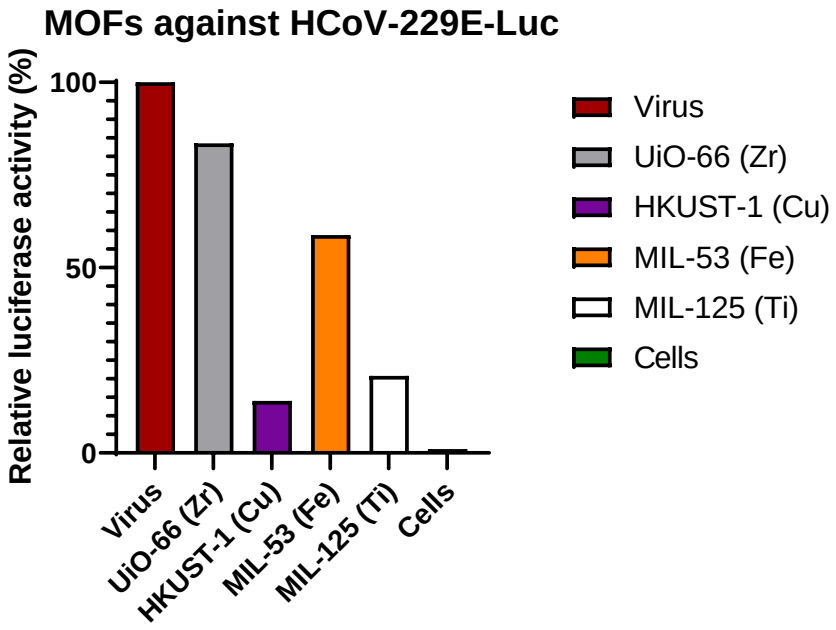

Figure 5. Results from the infection experiments with the MOFs against HCoV-229E (N = 3). After applying a two-way ANOVA and a Tukey's test, no statistically significant importance (ns) was found between the viral titer before and after the contact of the MOFs with the virus.

3.4 Results from the infection tests with SARS-CoV-2

In order to evaluate the effectiveness of the MOFs against SARS-CoV-2, three experiments were realized as described earlier, although this time two approaches of analyzing the results were applied, corresponding to the detection of viral protein N using western blot assay and the $TCID_{50}$ methods. For this purpose, a fifth MOF, MIL-125-NH_2 (Ti), was added to the study so as to be able to compare our results with the literature and prior to infection tests, its cytotoxicity was assessed (Figure S5). The five MOFs were tested at 1 and 5 mg/mL, except HKUST-1 (Cu), were we selected 0.1 mg/mL and 1 mg/mL. Two different controls were used as comparison media for the efficacy, a negative control with the virus without being in contact with any material and a positive control, where 1 mg/mL of HKUST-1 (Cu) - known to be toxic for the cells - was used. By comparing the controls, the intensity of the bands obtained with the anti-tubulin antibody is used to assess cell viability (Figure 6, anti-tubulin line), while that obtained with the anti-N antibody evaluates the effect of the MOF on viral infectivity (Figure 6, anti-N protein). When there is a signal (black rounded rectangle band), it means that either the cell viability is really high (anti-tubulin) or that the infection that took place was high (anti-N protein), while their absence means that the MOF compound was toxic to the cells or to the virus, respectively. By looking at the western blots, an effect with HKUST-1 (Cu) is seen at 0.1 mg/mL and a smaller effect with MIL-53 (Fe) and MIL-125 (Ti) at 5 mg/mL for the first experiment (N = 1) but was not confirmed in the other two experiments, N = 2 and 3. UiO-66 (Zr) and MIL-125(Ti)-NH_2 seem that they do not decrease the infectivity of the virus for all three experiments. Western blot seems not to give reproductive. Results for HKUST-1 (Cu), MIL-53 (Fe) and MIL-125 (Ti) obtained using western blot assays were not reproducible, thus the effects of MOF were evaluated using the $TCID_{50}$ method.

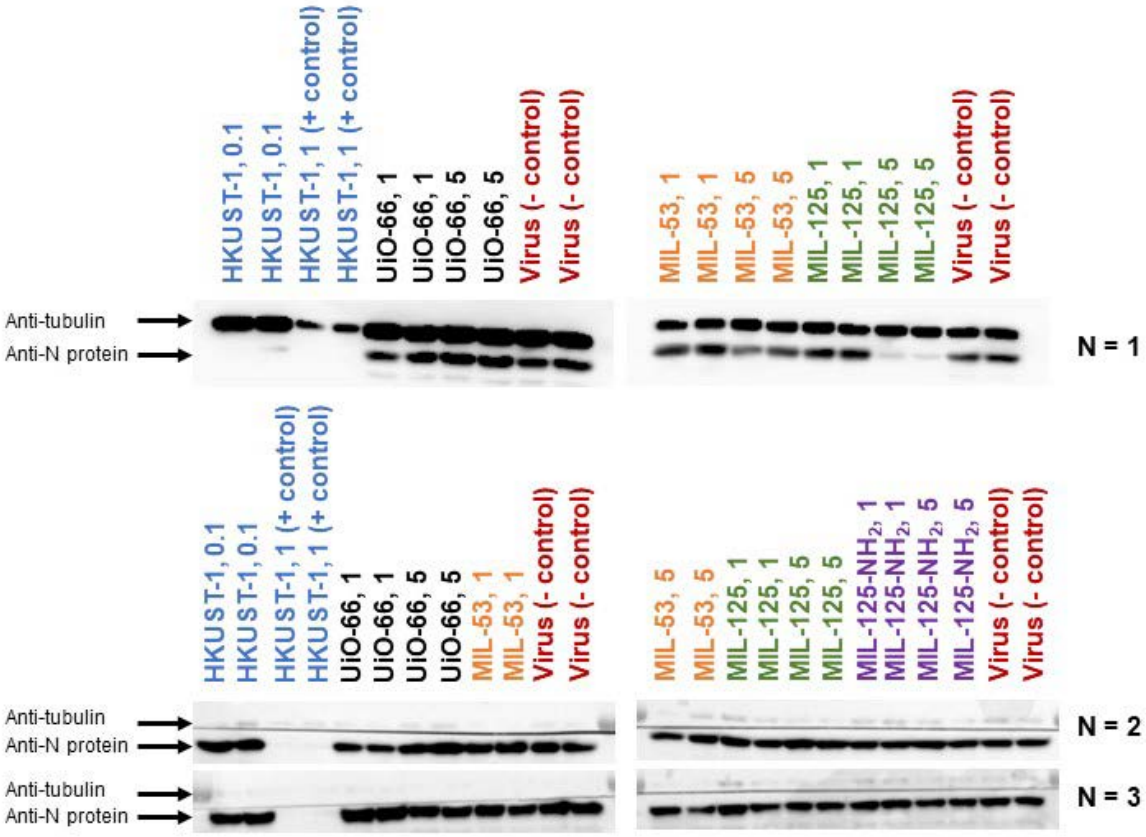

Figure 6. Western blots of the anti-tubulin (cells viability control) and anti-N protein of SARS-CoV-2. The numbers 0.1, 1 and 5 stated after each MOF represent their concentration in mg/mL. Each experiment done is noted by a number on the right-hand of the image, by N = 1, 2 or 3. Each measurement is repeated twice.

Regarding the results from the $TCID_{50}$ method (Figure 7), the reduction of the viral infectivity was calculated and expressed as a percentage of relative $TCID_{50}$ by dividing the value obtained from the MOF by the negative control (virus). For these experiments, 5 mg/mL was selected as the concentration of the MOFs, except of HKUST-1 (Cu) that was 0.1 mg/mL. This method is more sensitive for calculating the percentage of decrease of the viral titer, when that is between 1-100%. The best performing MOFs for inactivating SARS-CoV-2 are HKUST-1 (Cu),

MIL-53 (Fe) and UiO-66 (Zr) with an efficacy of 68.4%, 63.1% and 56.1%. Their antiviral effect against SARS-CoV-2 could be the same as observed for HCoV-229E and assigned to the catalytic degradation of the organic species. Although the structure of the viral particles is the same, there are differences that can explain why the same MOFs do not exhibit the same results on the two selected coronaviruses. The main differences lie in the recognition of cellular receptors to bind and enter the host cell, namely APN for HCoV-229E and ACE2 for SARS-CoV-2, or in the cleavage of glycoprotein Spike by cellular proteases after virus attachment.[7, 8, 64]. The two Ti-MOFs, MIL-125 (Ti) and MIL-125(Ti)-NH_2 show no effect against the virus, and confirmed a previous result.[48] Taken together, UiO-66 (Zr), HKUST-1 (Cu) and MIL-53 (Fe) decrease the infectivity of SARS-CoV-2, but the exact mechanism is not yet known and should be supplemented with further characterizations.

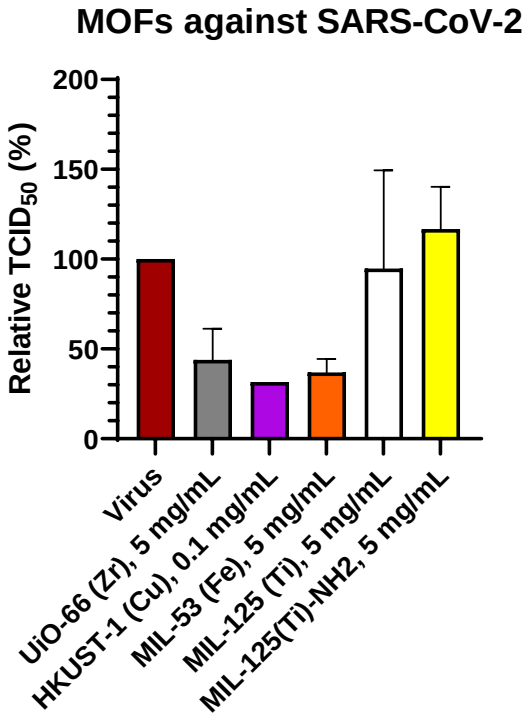

Figure 7. Results from the infection experiments with the MOFs against SARS-CoV-2 from the $TCID_{50}$ method (N = 3).

4. Conclusions

In summary, five Metal-Organic Frameworks were evaluated as coronavirucides. Firstly, their effect on cell viability was assessed using three of the most widely used cytotoxicity assays, in order to determine the concentrations to be tested for virucidicity The Neutral Red assay was found to be the most precise within the three, showing standard deviations of 0.4-25.2%. The results obtained were confirmed by the other two methods for MOFs on the 3 cell lines tested. HKUST-1 seems to be toxic in concentrations above 0.1 mg/mL for all three cell lines, while the other three materials can be used at higher concentrations above 1 mg/mL, probably due to its poor stability in aqueous media, that could release copper ions, which are cytotoxic.

Next, the highest safe concentration of each MOF for the appropriate cell lines was used to test their efficacy against two coronaviruses, HCoV-229E and SARS-CoV-2, by allowing the contact between the viruses and the MOF in an aqueous-based medium. HKUST-1 (Cu) and MIL-125 (Ti) reduce infectivity of HCoV-229E by 86% and 79.2% MIL-125 (Ti) was observed respectively. Concerning SARS-CoV-2, HKUST-1 (Cu) exhibits similar results than with HCoV-229E, although UiO-66 (Zr) and MIL-53 (Fe) show a higher decrease (≈65%) on the infectivity. Western blot was found to be less sensitive for this kind of measurement of the efficacy of MOFs than $TCID_{50}$, which gave accurate results. The same MOFs have differences in the inactivation activity towards each virus, which might depend on the different chemical composition of these two viruses. HKUST-1's activity could be attributed to the release of Cu(II) ions, that could either attack the viral proteins or the RNA of the virus, MIL-53's to the possible production of ROS,

while the Ti-based MOFs show dissimilar effect. Further studies need to be conducted on the mechanisms lying behind their activity.

ASSOCIATED CONTENT

Supporting Information.

MOFs syntheses and characterizations, cell culture protocol, cytotoxicity assay protocols.

AUTHOR INFORMATION

Corresponding Authors

christophe.volkringer@centralelille.fr

Author Contributions

The manuscript was written through contributions of all authors. All authors have given approval to the final version of the manuscript.

Funding Sources

This work was partially supported by the PEARL program (Program for Early-stage Researchers in Lille).

Note

The authors declare no competing financial interest.

Acknowledgments

The authors would like to thank Laurence Burylo and Philippe Devaux for their assistances with the synthesis and XRD powder patterns measurements (UCCS). The "Fonds Européen de

Développement Régional (FEDER)", "CNRS", "Région Hauts de France" and "Ministère de l'Education Nationale de l'Enseignement Supérieur et de la Recherche" are acknowledged for the funding of X-ray diffractometers and Scanning electron Microscopes from the Chevreul Institute platform. O.E. Plastiras thanks I-SITE ULNE for the fund from the program PEARL (Program for Early-stage Researchers in Lille), financed by the Marie Skłodowska-Curie Actions, from the H2020 program of the European Commission (Agreement N° 847569).

ABBREVIATIONS

MOF, Metal-Organic Framework; SARS-CoV-2, Severe Acute Respiratory Syndrome coronavirus 2

REFERENCES

(1) McKee, D. L.; Sternberg, A.; Stange, U.; Laufer, S.; Naujokat, C. Candidate drugs against SARS-CoV-2 and COVID-19. *Pharmacol. Res.* **2020**, *157*. DOI: 10.1016/j.phrs.2020.104859.
(2) Zheng, J. SARS-CoV-2: an Emerging Coronavirus that Causes a Global Threat. *Int. J. Biol. Sci.* **2020**, *16* (10), 1678-1685. DOI: 10.7150/ijbs.45053.
(3) Wang, H. H.; Li, X. M.; Li, T.; Zhang, S. B.; Wang, L. Z.; Wu, X.; Liu, J. Q. The genetic sequence, origin, and diagnosis of SARS-CoV-2. *Eur. J. Clin. Microbiol. Infect. Dis.* **2020**, *39* (9), 1629-1635. DOI: 10.1007/s10096-020-03899-4.
(4) World Health Organization (WHO). Coronavirus disease 2019 (COVID-19) Situation Report 150. https://www.who.int/publications/m/item/weekly-epidemiological-update-on-covid-19---6-july-2023 (accessed July 09, 2023).
(5) Comber, L.; Murchu, E. O.; Drummond, L.; Carty, P. G.; Walsh, K. A.; De Gascun, C. F.; Connolly, M. A.; Smith, S. M.; O'Neill, M.; Ryan, M.; et al. Airborne transmission of SARS-CoV-2 via aerosols. *Rev Med Virol.* **2021**, *31* (3). DOI: 10.1002/rmv.2184.
(6) Qian, H.; Miao, T.; Liu, L.; Zheng, X. H.; Luo, D. T.; Li, Y. G. Indoor transmission of SARS-CoV-2. *Indoor Air* **2021**, *31* (3), 639-645. DOI: 10.1111/ina.12766.
(7) Medina-Enriquez, M. M.; Lopez-Leon, S.; Carlos-Escalante, J. A.; Aponte-Torres, Z.; Cuapio, A.; Wegman-Ostrosky, T. ACE2: the molecular doorway to SARS-CoV-2. *Cell Biosci.* **2020**, *10* (1). DOI: 10.1186/s13578-020-00519-8.
(8) Scialo, F.; Daniele, A.; Amato, F.; Pastore, L.; Matera, M. G.; Cazzola, M.; Castaldo, G.; Bianco, A. ACE2: The Major Cell Entry Receptor for SARS-CoV-2. *Lung* **2020**, *198* (6), 867-877. DOI: 10.1007/s00408-020-00408-4.

(9) Lavie, M.; Dubuisson, J.; Belouzard, S. SARS-CoV-2 Spike Furin Cleavage Site and S2 ' Basic Residues Modulate the Entry Process in a Host Cell-Dependent Manner. *Journal of Virology* **2022**, *96* (13). DOI: 10.1128/jvi.00474-22.
(10) Bonnin, A.; Danneels, A.; Dubuisson, J.; Goffard, A.; Belouzard, S. HCoV-229E spike protein fusion activation by trypsin-like serine proteases is mediated by proteolytic processing in the S2 ' region. *Journal of General Virology* **2018**, *99* (7), 908-912. DOI: 10.1099/jgv.0.001074.
(11) Peacock, T. P.; Goldhill, D. H.; Zhou, J.; Baillon, L.; Frise, R.; Swann, O. C.; Kugathasan, R.; Penn, R.; Brown, J. C.; Sanchez-David, R. Y.; et al. The furin cleavage site in the SARS-CoV-2 spike protein is required for transmission in ferrets. *Nature Microbiology* **2021**, *6* (7), 899-+. DOI: 10.1038/s41564-021-00908-w.
(12) Amanat, F.; Krammer, F. SARS-CoV-2 Vaccines: Status Report. *Immunity* **2020**, *52* (4), 583-589. DOI: 10.1016/j.immuni.2020.03.007.
(13) Li, H. O.; Zhou, Y. J.; Zhang, M.; Wang, H. Z.; Zhao, Q.; Liu, J. Updated Approaches against SARS-CoV-2. *Antimicrob. Agents Chemother.* **2020**, *64* (6). DOI: 10.1128/aac.00483-20.
(14) Fukuda, M.; Islam, M. S.; Shimizu, R.; Nasser, H.; Rabin, N. N.; Takahashi, Y.; Sekine, Y.; Lindoy, L. F.; Fukuda, T.; Ikeda, T.; et al. Lethal Interactions of SARS-CoV-2 with Graphene Oxide: Implications for COVID-19 Treatment. *Acs Applied Nano Materials* **2021**, *4* (11), 11881-11887. DOI: 10.1021/acsanm.1c02446.
(15) Page, T. M.; Nie, C. X.; Neander, L.; Povolotsky, T. L.; Sahoo, A. K.; Nickl, P.; Adler, J. M.; Bawadkji, O.; Radnik, J.; Achazi, K.; et al. Functionalized Fullerene for Inhibition of SARS-CoV-2 Variants. *Small* **2023**, *19* (15). DOI: 10.1002/smll.202206154.
(16) Sarkar, P. K.; Mukhopadhyay, C. D. Ayurvedic metal nanoparticles could be novel antiviral agents against SARS-CoV-2. *International Nano Letters* **2021**, *11* (3), 197-203. DOI: 10.1007/s40089-020-00323-9.
(17) Jeremiah, S. S.; Miyakawa, K.; Morita, T.; Yamaoka, Y.; Ryo, A. Potent antiviral effect of silver nanoparticles on SARS-CoV-2. *Biochemical and Biophysical Research Communications* **2020**, *533* (1), 195-200. DOI: 10.1016/j.bbrc.2020.09.018.
(18) Tortella, G. R.; Pieretti, J. C.; Rubilar, O.; Fernandez-Baldo, M.; Benavides-Mendoza, A.; Diez, M. C.; Seabra, A. B. Silver, copper and copper oxide nanoparticles in the fight against human viruses: progress and perspectives. *Critical Reviews in Biotechnology* **2022**, *42* (3), 431-449. DOI: 10.1080/07388551.2021.1939260.
(19) Gkaniatsou, E.; Sicard, C.; Ricoux, R.; Mahy, J. P.; Steunou, N.; Serre, C. Metal-organic frameworks: a novel host platform for enzymatic catalysis and detection. *Mater. Horizons* **2017**, *4* (1), 55-63. DOI: 10.1039/c6mh00312e.
(20) Dhainaut, J.; Bonneau, M.; Ueoka, R.; Kanamori, K.; Furukawa, S. Formulation of Metal-Organic Framework Inks for the 3D Printing of Robust Microporous Solids toward High-Pressure Gas Storage and Separation. *ACS Appl. Mater. Interfaces* **2020**, *12* (9), 10983-10992. DOI: 10.1021/acsami.9b22257.
(21) Leloire, M.; Dhainaut, J.; Devaux, P.; Leroy, O.; Desjonqueres, H.; Poirier, S.; Nerisson, P.; Cantrel, L.; Royer, S.; Loiseau, T.; et al. Stability and radioactive gaseous iodine-131 retention capacity of binderless UiO-66-NH2 granules under severe nuclear accidental conditions. *J. Hazard. Mater.* **2021**, *416*. DOI: 10.1016/j.jhazmat.2021.125890.
(22) Shen, K.; Chen, X. D.; Chen, J. Y.; Li, Y. W. Development of MOF-Derived Carbon-Based Nanomaterials for Efficient Catalysis. *ACS Catal.* **2016**, *6* (9), 5887-5903. DOI: 10.1021/acscatal.6b01222.

(23) Manousi, N.; Plastiras, O. E.; Kalogiouri, N. P.; Zacharis, C. K.; Zachariadis, G. A. Metal-Organic Frameworks in Bioanalysis: Extraction of Small Organic Molecules. *Separations* **2021**, *8* (5). DOI: 10.3390/separations8050060.
(24) Sava Gallis, D. F.; Rohwer, L. E. S.; Rodriguez, M. A.; Barnhart -Dailey, M. C.; Butler, K. S.; Luk, T. S.; Timlin, J. A.; Chapman, K. W. Multifunctional, Tunable Metal-Organic Framework Materials Platform for Bioimaging Applications. *ACS Appl. Mater. Interfaces* **2017**, *9* (27), 22268-22277. DOI: 10.1021/acsami.7b05859.
(25) Gimenez-Marques, M.; Hidalgo, T.; Serre, C.; Horcajada, P. Nanostructured metal-organic frameworks and their bio-related applications. *Coord. Chem. Rev* **2016**, *307*, 342-360. DOI: 10.1016/j.ccr.2015.08.008.
(26) Horcajada, P.; Serre, C.; Maurin, G.; Ramsahye, N. A.; Balas, F.; Vallet-Regi, M.; Sebban, M.; Taulelle, F.; Ferey, G. Flexible porous metal-organic frameworks for a controlled drug delivery. *Journal of the American Chemical Society* **2008**, *130* (21), 6774-6780. DOI: 10.1021/ja710973k.
(27) Mallakpour, S.; Nikkhoo, E.; Hussain, C. M. Application of MOF materials as drug delivery systems for cancer therapy and dermal treatment. *Coordination Chemistry Reviews* **2022**, *451*. DOI: 10.1016/j.ccr.2021.214262.
(28) Malich, G.; Markovic, B.; Winder, C. The sensitivity and specificity of the MTS tetrazolium assay for detecting the in vitro cytotoxicity of 20 chemicals using human cell lines. *Toxicology* **1997**, *124* (3), 179-192. DOI: 10.1016/s0300-483x(97)00151-0.
(29) Chandra, R.; Singh, V.; Tomar, S.; Nath, M. Multi-core-shell composite SnO(2)NPs@ZIF-8: potential antiviral agent and effective photocatalyst for waste-water treatment. *Environ. Sci. Pollut. Res.* **2019**, *26* (23), 23346-23358. DOI: 10.1007/s11356-019-05646-5.
(30) Motakef-Kazemi, N.; Shojaosadati, S. A.; Morsali, A. Evaluation of the effect of nanoporous nanorods Zn-2(bdc)(2)(dabco) dimension on ibuprofen loading and release. *J. Iran. Chem. Soc.* **2016**, *13* (7), 1205-1212. DOI: 10.1007/s13738-016-0835-9.
(31) Ates, G.; Vanhaecke, T.; Rogiers, V.; Rodrigues, R. M. Assaying Cellular Viability Using the Neutral Red Uptake Assay. *Cell Viability Assays: Methods and Protocols* **2017**, *1601*, 19-26. DOI: 10.1007/978-1-4939-6960-9_2.
(32) Valdiviesogarcia, A.; Clarke, R. C.; Rahn, K.; Durette, A.; Macleod, D. L.; Gyles, C. L. NEUTRAL RED ASSAY FOR MEASUREMENT OF QUANTITATIVE VERO CELL CYTOTOXICITY. *Appl. Environ. Microbiol.* **1993**, *59* (6), 1981-1983. DOI: 10.1128/aem.59.6.1981-1983.1993.
(33) Olabarrieta, I.; L'Azou, B.; Yuric, S.; Cambar, J.; Cajaraville, M. P. In vitro effects of cadmium on two different animal cell models. *Toxicol. In Vitro* **2001**, *15* (4-5), 511-517. DOI: 10.1016/s0887-2333(01)00056-x.
(34) Fotakis, G.; Timbrell, J. A. In vitro cytotoxicity assays: Comparison of LDH, neutral red, MTT and protein assay in hepatoma cell lines following exposure to cadmium chloride. *Toxicol. Lett.* **2006**, *160* (2), 171-177. DOI: 10.1016/j.toxlet.2005.07.001.
(35) Chen, G. S.; Leng, X.; Luo, J. Y.; You, L. T.; Qu, C. H.; Dong, X. V.; Huang, H. L.; Yin, X. B.; Ni, J. In Vitro Toxicity Study of a Porous Iron(III) Metal-Organic Framework. *Molecules* **2019**, *24* (7). DOI: 10.3390/molecules24071211.
(36) Jarai, B. M.; Stillman, Z.; Attia, L.; Decker, G. E.; Bloch, E. D.; Fromen, C. A. Evaluating UiO-66 Metal-Organic Framework Nanoparticles as Acid-Sensitive Carriers for Pulmonary Drug Delivery Applications. *ACS Appl. Mater. Interfaces* **2020**, *12* (35), 38989-39004. DOI: 10.1021/acsami.0c10900.

(37) Dymek, K.; Kurowski, G.; Kuterasinski, L.; Jedrzejczyk, R.; Szumera, M.; Sitarz, M.; Pajdak, A.; Kurach, L.; Boguszewska-Czubara, A.; Jodlowski, P. J. In Search of Effective UiO-66 Metal-Organic Frameworks for Artificial Kidney Application. *ACS Appl. Mater. Interfaces* **2021**, *13* (38), 45149-45160. DOI: 10.1021/acsami.1c05972.
(38) Motakef-Kazemi, N.; Shojaosadati, S. A.; Morsali, A. In situ synthesis of a drug-loaded MOF at room temperature. *Microporous Mesoporous Mater* **2014**, *186*, 73-79. DOI: 10.1016/j.micromeso.2013.11.036.
(39) Ruyra, A.; Yazdi, A.; Espin, J.; Carne-Sanchez, A.; Roher, N.; Lorenzo, J.; Imaz, I.; Maspoch, D. Synthesis, Culture Medium Stability, and In Vitro and In Vivo Zebrafish Embryo Toxicity of Metal-Organic Framework Nanoparticles. *Chem. Eur. J.* **2015**, *21* (6), 2508-2518. DOI: 10.1002/chem.201405380.
(40) Wang, J. Q.; Chen, D. M.; Li, B.; He, J.; Duan, D. L.; Shao, D. D.; Nie, M. F. Fe-MIL-101 exhibits selective cytotoxicity and inhibition of angiogenesis in ovarian cancer cells via downregulation of MMP. *Sci. Rep.* **2016**, *6*. DOI: 10.1038/srep26126.
(41) Tamames-Tabar, C.; Cunha, D.; Imbuluzqueta, E.; Ragon, F.; Serre, C.; Blanco-Prieto, M. J.; Horcajada, P. Cytotoxicity of nanoscaled metal-organic frameworks. *J Mater Chem B* **2014**, *2* (3), 262-271. DOI: 10.1039/c3tb20832j.
(42) Abramenko, N.; Deyko, G.; Abkhalimov, E.; Isaeva, V.; Pelgunova, L.; Krysanov, E.; Kustov, L. Acute Toxicity of Cu-MOF Nanoparticles (nanoHKUST-1) towards Embryos and Adult Zebrafish. *Int. J. Mol. Sci* **2021**, *22* (11). DOI: 10.3390/ijms22115568.
(43) Almasi, M. A review on state of art and perspectives of Metal-Organic frameworks (MOFs) in the fight against coronavirus SARS-CoV-2. *J Coord Chem* **2021**, *74* (13), 2111-2127. DOI: 10.1080/00958972.2021.1965130.
(44) Cheung, Y. H.; Ma, K. K.; van Leeuwen, H. C.; Wasson, M. C.; Wang, X. J.; Idrees, K. B.; Gong, W.; Cao, R.; Mahle, J. J.; Islamoglu, T.; et al. Immobilized Regenerable Active Chlorine within a Zirconium-Based MOF Textile Composite to Eliminate Biological and Chemical Threats. *Journal of the American Chemical Society* **2021**, *143* (40), 16777-16785. DOI: 10.1021/jacs.1c08576.
(45) Kumar, A.; Soni, V.; Singh, P.; Khan, A. A. P.; Nazim, M.; Mohapatra, S.; Saini, V.; Raizada, P.; Hussain, C. M.; Shaban, M.; et al. Green aspects of photocatalysts during corona pandemic: a promising role for the deactivation of COVID-19 virus. *Rsc Adv.* **2022**, *12* (22), 13609-13627. DOI: 10.1039/d1ra08981a.
(46) Wang, X. J.; Ma, K. K.; Goh, T.; Mian, M. R.; Xie, H. M.; Mao, H. C.; Duan, J. X.; Kirlikovali, K. O.; Stone, A.; Ray, D.; et al. Photocatalytic Biocidal Coatings Featuring Zr6Ti4-Based Metal-Organic Frameworks. *J. Am. Chem. Soc.* **2022**, *144* (27), 12192-12201. DOI: 10.1021/jacs.2c03060.
(47) Givirovskaia, D.; Givirovskiy, G.; Haapakoski, M.; Hokkanen, S.; Ruuskanen, V.; Salo, S.; Marjomaki, V.; Ahola, J.; Repo, E. Modification of face masks with zeolite imidazolate framework-8: A tool for hindering the spread of COVID-19 infection. *Microporous Mesoporous Mater* **2022**, *334*. DOI: 10.1016/j.micromeso.2022.111760.
(48) Ornstein, J.; Ozdemir, R. O. K.; Boehme, A.; Nouar, F.; Serre, C.; Ackerman, D. N.; Herrera, V. L.; Santarpia, J. L. SARS-CoV-2 Inactivation Potential of Metal Organic Framework

Induced Photocatalysis. 2020.
(49) van den Worm, S. H. E.; Eriksson, K. K.; Zevenhoven, J. C.; Weber, F.; Zust, R.; Kuri, T.; Dijkman, R.; Chang, G. H.; Siddell, S. G.; Snijder, E. J.; et al. Reverse Genetics of SARS-

Related Coronavirus Using Vaccinia Virus-Based Recombination. *PLoS One* **2012**, *7* (3). DOI: 10.1371/journal.pone.0032857.
(50) Meunier, T.; Desmarets, L.; Bordage, S.; Bamba, M.; Hervouet, K.; Rouille, Y.; Francois, N.; Decossas, M.; Sencio, V.; Trottein, F.; et al. A Photoactivable Natural Product with Broad Antiviral Activity against Enveloped Viruses, Including Highly Pathogenic Coronaviruses. *Antimicrob. Agents Chemother.* **2022**, *66* (2). DOI: 10.1128/aac.01581-21.
(51) Meunier, T.; Desmarets, L.; Bordage, S.; Bamba, M.; Hervouet, K.; Rouille, Y.; Francois, N.; Decossas, M.; Sencio, V.; Trottein, F.; et al. A Photoactivable Natural Product with Broad Antiviral Activity against Enveloped Viruses, Including Highly Pathogenic Coronaviruses. *Antimicrobial Agents and Chemotherapy* **2022**, *66* (2). DOI: 10.1128/aac.01581-21.
(52) R Core Team (2022), R. A language and environment for statistical computing, R Foundation for Statistical Computing. Vienna, Austria.
(53) Calland, N.; Sahuc, M. E.; Belouzard, S.; Pene, V.; Bonnafous, P.; Mesalam, A. A.; Deloison, G.; Descamps, V.; Sahpaz, S.; Wychowski, C.; et al. Polyphenols Inhibit Hepatitis C Virus Entry by a New Mechanism of Action. *Journal of Virology* **2015**, *89* (19), 10053-10063. DOI: 10.1128/jvi.01473-15.
(54) Millet, J. K.; Seron, K.; Labitt, R. N.; Danneels, A.; Palmer, K. E.; Whittaker, G. R.; Dubuisson, J.; Belouzard, S. Middle East respiratory syndrome coronavirus infection is inhibited by griffithsin. *Antiviral Research* **2016**, *133*, 1-8. DOI: 10.1016/j.antiviral.2016.07.011.
(55) Warnes, S. L.; Little, Z. R.; Keevil, C. W. Human Coronavirus 229E Remains Infectious on Common Touch Surface Materials. *Mbio* **2015**, *6* (6). DOI: 10.1128/mBio.01697-15.
(56) Husain, N.; Mahmood, R. Copper(II) generates ROS and RNS, impairs antioxidant system and damages membrane and DNA in human blood cells. *Environmental Science and Pollution Research* **2019**, *26* (20), 20654-20668. DOI: 10.1007/s11356-019-05345-1.
(57) Giovine, R.; Pourpoint, F.; Duval, S.; Lafon, O.; Amoureux, J. P.; Loiseau, T.; Volkringer, C. The Surprising Stability of Cu₃(btc)₂ Metal-Organic Framework under Steam Flow at High Temperature. *Crystal Growth & Design* **2018**, *18* (11), 6681-6693. DOI: 10.1021/acs.cgd.8b00931.
(58) Vincent, M.; Duval, R. E.; Hartemann, P.; Engels-Deutsch, M. Contact killing and antimicrobial properties of copper. *Journal of Applied Microbiology* **2018**, *124* (5), 1032-1046. DOI: 10.1111/jam.13681.
(59) Butot, S.; Baert, L.; Zuber, S. Assessment of Antiviral Coatings for High-Touch Surfaces by Using Human Coronaviruses HCoV-229E and SARS-CoV-2. *Applied and Environmental Microbiology* **2021**, *87* (19). DOI: 10.1128/aem.01098-21.
(60) Kim, S. N.; Kim, J.; Kim, H. Y.; Cho, H. Y.; Ahn, W. S. Adsorption/catalytic properties of MIL-125 and NH2-MIL-125. *Catalysis Today* **2013**, *204*, 85-93. DOI: 10.1016/j.cattod.2012.08.014.
(61) McNamara, N. D.; Neumann, G. T.; Masko, E. T.; Urban, J. A.; Hicks, J. C. Catalytic performance and stability of (V) MIL-47 and (Ti) MIL-125 in the oxidative desulfurization of heterocyclic aromatic sulfur compounds. *Journal of Catalysis* **2013**, *305*, 217-226. DOI: 10.1016/j.jcat.2013.05.021.
(62) Li, A. X.; Yang, X. X.; Chen, J. A novel route to size-controlled MIL-53(Fe) metal-organic frameworks for combined chemodynamic therapy and chemotherapy for cancer. *Rsc Advances* **2021**, *11* (18), 10540-10547. DOI: 10.1039/d0ra09915e.
(63) Chen, H.; Liu, Y. T.; Cai, T.; Dong, W. Y.; Tang, L.; Xia, X. N.; Wang, L. L.; Li, T. Boosting Photocatalytic Performance in Mixed-Valence MIL-53(Fe) by Changing Fe-II/Fe-III

Ratio. *Acs Applied Materials & Interfaces* **2019**, *11* (32), 28791-28800. DOI: 10.1021/acsami.9b05829.
(64) Fehr, A. R.; Perlman, S. Coronaviruses: An Overview of Their Replication and Pathogenesis. *Coronaviruses: Methods and Protocols* **2015**, *1282*, 1-23. DOI: 10.1007/978-1-4939-2438-7_1.